A novel isoform of the Ly108 gene ameliorates murine lupus

Marton Keszei,[1] Cynthia Detre,[1] Svend T. Rietdijk,[1] Pilar Muñoz,[2] Xavier Romero,[1] Scott B. Berger,[1] Silvia Calpe,[1] Gongxian Liao,[1] Wilson Castro,[1] Aimee Julien,[1] Ying-Yu Wu,[1] Dong-Mi Shin,[3] Jaime Sancho,[2] Mercedes Zubiaur,[2] Herbert C. Morse III,[3] Laurence Morel,[4] Pablo Engel,[5] Ninghai Wang,[1] and Cox Terhorst[1]

[1]Division of Immunology, Department of Medicine, Beth Israel Deaconess Medical Center, Harvard Medical School, Boston, MA 02115
[2]Instituto de Parasitología y Biomedicina, Consejo Superior de Investigaciones Científicas, 18100 Armilla, Granada, Spain
[3]Laboratory of Immunopathology, National Institute of Allergy and Infectious Diseases, National institutes of Health, Rockville, MD 20852
[4]Department of Pathology, Immunology, and Laboratory Medicine, University of Florida College of Medicine, Gainesville, FL 32610
[5]Immunology Unit, Department of Cellular Biology and Pathology, Medical School, University of Barcelona, 08036 Barcelona, Spain

Studies of human systemic lupus erythematosus patients and of murine congenic mouse strains associate genes in a DNA segment on chromosome 1 with a genetic predisposition for this disease. The systematic analysis of lupus-prone congenic mouse strains suggests a role for two isoforms of the Ly108 receptor in the pathogenesis of the disease. In this study, we demonstrate that Ly108 is involved in the pathogenesis of lupus-related autoimmunity in mice. More importantly, we identified a third protein isoform, Ly108-H1, which is absent in two lupus-prone congenic animals. Introduction of an Ly108-H1–expressing transgene markedly diminishes T cell–dependent autoimmunity in congenic *B6.Sle1b* mice. Thus, an immune response–suppressing isoform of Ly108 can regulate the pathogenesis of lupus.

CORRESPONDENCE
Cox Terhorst:
cterhors@bidmc.harvard.edu
OR
Marton Keszei:
mkeszei@bidmc.harvard.edu

Abbreviations used: ANA, antinuclear antibody; BAC, bacterial artificial chromosome; dsDNA, double-stranded DNA; ES, embryonic stem; ITSM, immuno-tyrosine switch motif; mRNA, messenger RNA; PNGaseF, peptide: *N*-glycosidase F; SAP, SLAM-associated protein; SLAM, signaling lymphocytic activation molecule; SLAMF, SLAM family; SLE, systemic lupus erythematosus; SNP, single nucleotide polymorphism; ssDNA, single-stranded DNA.

Systemic lupus erythematosus (SLE) is a chronic autoimmune disease characterized by the production of autoantibodies against a wide spectrum of self-antigens, especially from the cell nucleus. Genes in multiple pathways participate in mediating disease pathogenesis, and epistatic interactions among these genes influence the severity of disease. SLE-related genes include, for instance, those involved in physiological pathways of waste disposal mechanisms, regulating the removal of circulating immune complexes and apoptotic cells by the mononuclear phagocyte system, or those involved in T cell functions. Several of the signaling lymphocytic activation molecule (SLAM) family (SLAMF) genes, which encode cell surface receptors and which affect both antigen-presenting cell and T cell functions, may also regulate thresholds for tolerance and activation of T and B lymphocytes as well as reactivation-induced cell death (Wandstrat et al., 2004; Kumar et al., 2006; Carlucci et al., 2007; Calpe et al., 2008; Cunninghame Graham et al., 2008; Snow et al., 2009; Detre et al., 2010; Kim et al., 2010; Morel, 2010; You et al., 2010).

In mice, the SLAMF cell surface receptors encode nine genes (*Slamf1–9*; Calpe et al., 2008) that vary between two sets of mouse strains: *Slamf*-haplotype 1, e.g., *C57BL/6* (*B6*), and *Slamf*-haplotype 2, e.g., *NZW* or *129* (Wandstrat et al., 2004; Detre et al., 2010). In the lupus-prone congenic mouse strains, *B6.Sle1b* (*Sle1b*) and *B6.129chr1b*, DNA segments derived from *NZW* or *129*, respectively, are embedded in the *B6* genome. These *NZW* or *129* segments contain several genes, including *Slamf1–7*.

M. Keszei, C. Detre, and S.T. Rietdijk contributed equally to this paper.

The Rockefeller University Press $30.00
J. Exp. Med. Vol. 208 No. 4 811-822
www.jem.org/cgi/doi/10.1084/jem.20101653

Autoantibodies develop because of an epistatic interplay between one or more *Slamf*-haplotype 2 genes with *B6* genes (Bygrave et al., 2004; Wandstrat et al., 2004; Carlucci et al., 2007). Based on the studies with the *Sle1b* mouse (Wandstrat et al., 2004; Kumar et al., 2006), Ly108 (*Slamf6*) has been suggested as a candidate susceptibility gene for SLE. An initial study using *BALB/c* splenocytes identified two Ly108-coding cDNAs (Peck and Ruley, 2000), later termed Ly108-1 (GenBank/EMBL/DDBJ accession no. AF248635.1) and Ly108-2 (GenBank accession no. AF248636.1). These two splice variants of Ly108 are thought to encode protein isoforms with identical extracellular domains but differing cytoplasmic tails. The ratio of transcripts encoding Ly108-1 and Ly108-2 differs in *Sle1b* and *B6* lymphocytes, which is thought to influence early B cell development (Kumar et al., 2006), resulting in increased autoantibody production. The B cell experiments led to the conclusion that "the normal Ly108-2 allele, but not the lupus-associated Ly108-1 allele, was found to sensitize immature B cells to deletion and RAG re-expression" (Kumar et al., 2006).

In this study, we use gene-targeted mutant and congenic mice in combination with bacterial artificial chromosome (BAC)–based transgenic mice to provide evidence that Ly108 is involved in the regulation of SLE in a $CD4^+$ T cell–dependent manner. In addition to Ly108-1 and Ly108-2, we identify a novel protein isoform, Ly108-H1, which is present only in *Slamf*-haplotype 1 mice and not in the lupus-prone *Sle1b* or *B6.129chr1b* strains. Introduction of one copy of an Ly108-H1 BAC-based transgene into the *Sle1b* dramatically reduces lupus-related autoimmunity. Thus, although the *Slamf*-haplotype 2 segment in the congenic *Sle1b* mouse contains circa 20 genes, the Ly108-H1 isoform plays a dominant role in suppressing the pathogenesis of SLE.

RESULTS

The congenic Ly108$^{-/-}$ [*129* × *B6*] mouse does not develop SLE, in contrast to the *B6.129chr1b* congenic mouse, which contains the same *129*-derived segment

To examine whether disruption of the Ly108 gene would affect the development of murine lupus, we backcrossed our congenic Ly108$^{-/-}$ [*129* × *B6*] mouse, which was generated with *129*-derived embryonic stem (ES) cells (Howie et al., 2005), with the WT *B6* mouse. In addition, we generated a new *B6*.Ly108$^{-/-}$ mouse using *B6* ES cells (Fig. S1, A–D). We hypothesized that the congenic Ly108$^{-/-}$ [*129* × *B6*] mouse would not develop lupus if Ly108 played a dominant role in the pathogenesis of the disease. In contrast, Ly108$^{-/-}$ [*129* × *B6*] would develop disease if genes other than Ly108 that are present in the selected *129*-derived segment were of equal or greater importance.

We found that in aged Ly108$^{-/-}$ [*129* × *B6*] females, antinucleosome autoantibody levels were similar to those in *B6* mice, whereas these antibodies were detected in the serum of the lupus-prone *B6.129chr1b* [*129* × *B6*] and *Sle1b* [*NZW* × *B6*] mice. Furthermore, the *B6*.Ly108$^{-/-}$ mice also did not develop lupus (Fig. 1 A). As expected in the case of a T cell–dependent autoimmune disease (Crispín et al., 2010b), the percentage of effector/memory $CD4^+$ T cells was increased in aged *B6.129chr1b* and *Sle1b* mice (Fig. 1 B). In contrast, the percentage of effector/memory $CD4^+$ T cells

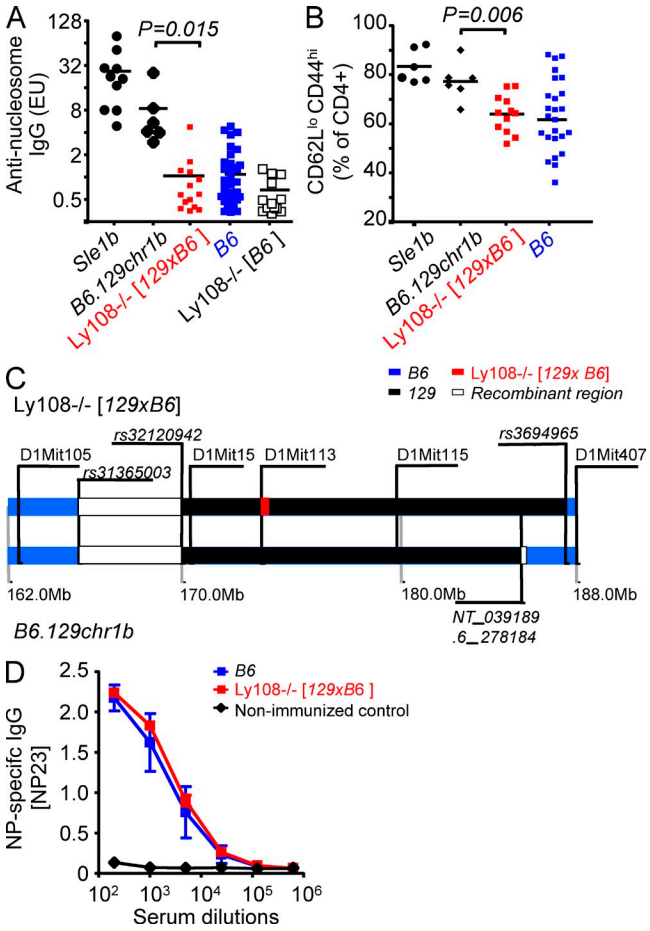

Figure 1. The Ly108$^{-/-}$ [*129* × *B6*] mouse does not develop SLE, in contrast to the *B6.129chr1b* congenic mouse, which contains a similar *129*-derived segment. (A) Antinucleosome antibodies in the serum of individual females (10–13 mo old) were determined, as indicated in Materials and methods. Mice were aged in the same animal facility, and sera were collected and stored at −80°C until analysis. *Sle1b*, $n = 10$; *B6.129chr1b*, $n = 6$; Ly108$^{-/-}$ [*129* × *B6*], $n = 14$; *B6*, $n = 38$; Ly108$^{-/-}$ [*B6*], $n = 13$. Mean titers are indicated by a horizontal line. EU, ELISA units. (B) Percentage of effector/memory $CD4^+$ cells was determined by flow cytometric analysis of the spleen of individual females (10–13 mo old) as described in Materials and methods. *Sle1b*, $n = 6$; *B6.129chr1b*, $n = 6$; Ly108$^{-/-}$ [*129* × *B6*], $n = 12$; *B6*, $n = 25$. Mean values are indicated by a horizontal line. (C) Congenic boundaries of the *129* segments on chromosome 1 of Ly108$^{-/-}$ [*129* × *B6*] and of *B6.129chr1b* mice were determined using the Mouse Diversity Genotyping array (Affymetrix) and microsatellite analysis. (D) Normal T cell–dependent humoral response in Ly108$^{-/-}$ [*129* × *B6*] mice. Ly108$^{-/-}$ [*129* × *B6*] and WT [*B6*] mice were immunized i.p. with 50 µg NP-KLH, and 14 d after immunization, serum titers were determined by ELISA using NP(23)-BSA–coated plates. The mean values and SDs of NP-specific IgG titers were determined using five mice/group. All statistical analyses in this figure were performed by the Mann-Whitney nonparametric, two-tailed test.

in the aged Ly108$^{-/-}$ [*129* × *B6*] mice was equivalent to that in WT *B6* mice (Fig. 1 B). Low-resolution microsatellite marker analysis of the boundaries of the *129*-derived segment in Ly108$^{-/-}$ [*129* × *B6*] and *B6.129chr1b* mice showed that they were similar (Fig. 1 C and Fig. S1 F). Support for the presence of the *129*-derived segment (e.g., *Slamf*-haplotype 2) in both mouse strains comes from staining with haplotype 2–specific α-Hap2 antibody (Fig. S1 E). To fine-map the exact breakpoint between the *B6* genetic background and the *129* congenic insert in Ly108$^{-/-}$ [*129* × *B6*] and *B6.129chr1b* mice, we used a single nucleotide polymorphism (SNP) genotyping microarray. Notably, on the centromeric side of the congenic insert, the first *129* SNP allele was rs32120942 (National Center for Biotechnology Information [NCBI] SNP database accession no.) for both the Ly108$^{-/-}$ [*129* × *B6*] and *B6.129chr1b* analysis (Fig. 1 C and Table S2). However, the exact breakpoint upstream of SNP rs32120942, which spans 4.8 Mb, could not be determined as no sequence differences among the 1,406 *B6* and *129* SNP alleles were included on the array. This observation argues that the centromeric side recombinant region belongs to an identical large haplotype block in *129* and *B6* mice; thus, there is no reason to attempt to find the exact breakpoint. On the telomeric side, the *129*-derived segment is 2 Mb longer in Ly108$^{-/-}$ [*129* × *B6*] than in *B6.129chr1b* and contains 18 RefSeq genes (Fig. S1 G). None of the possible differences between Ly108$^{-/-}$ [*129* × *B6*] and *B6.129chr1b* genomic sequence overlap with any of the described SLE suppressor regions in *129* or *NZW* (Morel et al., 1999; Subramanian et al., 2005). Thus, the disruption of the Ly108 gene in a congenic mouse ameliorates disease found in a very similar congenic mouse strain that harbors the intact *129*-derived Ly108 gene.

Because the homophilic receptor Ly108 is expressed on both T and B cells, we examined whether specific T cell–dependent antibody responses would be affected by the Ly108^{null} mutation. As shown in Fig. 1 D and Fig. S1 H, T cell–dependent low- and high-affinity antibody responses to haptenated proteins by the congenic Ly108$^{-/-}$ [*129* × *B6*] mice are identical to those by WT *B6* mice. We conclude that the absence of the lupus-susceptibility gene Ly108 significantly reduces antinucleosome antibody responses and CD4$^+$ T cell expansion in a *B6* mouse, which contains a short *129*-derived segment.

Protein isoform analysis detects Ly108-H1, a novel protein isoform, which is coexpressed with Ly108-1 and Ly108-2 in *Slamf*-haplotype 1 mice

Because the difference in expression levels of the two Ly108 alleles in the *Sle1b* and *B6* mouse was based on quantitative PCR (Wandstrat et al., 2004), we set out to examine whether the Ly108-1/2 isoform variability was reflected at the protein level of *Slamf*-haplotype 1 and 2 mice. First, we assessed the expression pattern of Ly108 on the surface of hematopoietic cells derived from known *Slamf*-haplotype 1 and 2 mice using our anti-Ly108 monoclonal antibody, 13G3, which is specific for the extracellular region of the receptor (Fig. 2 A). Surprisingly, CD4$^-$8$^-$ (double negative) and CD4$^+$8$^+$ (double positive) thymocyte subsets derived from the *Slamf*-haplotype 1 mice, *B6* and *MOLF/EiJ*, expressed considerably more Ly108 than thymocyte subsets isolated from *Slamf*-haplotype 2 mice, e.g., *BALB/c*, *129*, and *Sle1b* (Fig. 2 A).

The difference in Ly108 cell surface expression in *Slamf*-haplotype 1 mice appeared to be a reflection of increased transcription of the *Slamf6* gene, as judged by quantitative PCR (Fig. S2). We therefore evaluated whether the difference in cell surface expression among strains of the two *Slamf*-haplotypes could be attributed to an increase in Ly108 protein expression, particularly among the two isoforms. To this end, immunoprecipitates made with monoclonal α-Ly108 (13G3) were subjected to SDS-PAGE, and the protein isoforms Ly108-1 and Ly108-2 were identified by Western blotting with two polyclonal antibodies. One antibody (R4) was directed

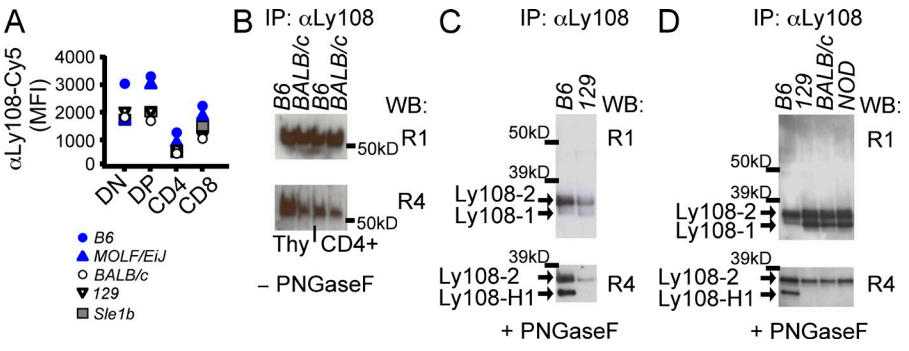

Figure 2. Ly108-H1, a novel protein isoform, is only expressed in *Slamf*-haplotype 1 mice. (A) Ly108 cell surface expression in *Slamf*-haplotype 1 and 2 T lineage cells was determined by flow cytometric analysis. The mean fluorescence intensity (MFI) is given as a mean of three animals in each group. Results are representative of four independent experiments. DN, double negative thymocytes; DP, double positive thymocytes. (B) Protein expression of Ly108 in lysates of thymocytes or splenic CD4$^+$ T cells isolated from *B6* and *BALB/c* mice. Anti-Ly108 immunoprecipitates were subjected to SDS-PAGE, and proteins were detected by Western blotting (WB) using either polyclonal antibody R1, which recognizes the cytoplasmic tails of both Ly108-1 and Ly108-2, or polyclonal antibody R4, which is directed against a peptide that is only present in the cytoplasmic tail of Ly108-2 (see also Fig. 3 D). The data are representative of two independent experiments. (C) Immunoprecipitates (IP: α-Ly108) from *B6* and *129* thymocytes were deglycosylated with PNGaseF before SDS-PAGE followed by Western blotting using R1 (top) and R4 (bottom) antibodies. The data are representative of two independent experiments. (D) Lysates of B cells isolated from the spleen of *B6*, *129*, *BALB/c*, and *NOD* mice by magnetic cell sorting were immunoprecipitated with anti-Ly108 and were subjected to PNGaseF treatment, SDS-PAGE, and Western blotting with R1 or R4. The figure shows a single analysis of four different mouse strains.

against a unique amino acid sequence in the C terminus of the Ly108-2 cytoplasmic tail and the second antibody (R1) against a cytoplasmic tail segment shared by the two isoforms (Fig. 3 D). The glycosylated Ly108-1 and Ly108-2 proteins, when precipitated from thymocytes and $CD4^+$ T cells of *B6* or *BALB/c* mice, ran as indistinguishable bands upon Western blotting with R1. However, when the immunoprecipitates were blotted with the R4 antibody, samples from *B6* mice consistently showed higher Ly108-2 expression as compared with the same cell subsets of the *BALB/c* animals (Fig. 2 B). Upon deglycosylation with the enzyme PNGaseF (peptide: *N*-glycosidase F), Ly108-1 and Ly108-2 protein isoforms migrated according to their predicted molecular masses, 34 kD and 36 kD, respectively (Fig. 2 C, top). Surprisingly, when the membranes were reprobed with the R4 antibody (Fig. 2 C, bottom), two proteins were detected in *B6* thymocytes. In addition to the 36-kD Ly108-2 protein, a smaller 30-kD protein, designated Ly108-H1, was present only in the *B6* thymocytes. The Ly108-H1 protein was also present in B lymphocytes of *B6* mice but not in *129*, *BALB/c*, or *NOD* B lymphocytes (Fig. 2 D).

Thus, the presence of a previously unidentified protein isoform, Ly108-H1, expressed exclusively in *Slamf*-haplotype 1 mouse strains, could, at least in part, have accounted for the elevated Ly108 expression in *B6* thymocytes. Because quantitation by Western blotting of immunoprecipitates is inherently difficult, a difference in protein expression of Ly108-1 and Ly108-2 could not be excluded.

The Ly108-H1 protein is encoded by a splice variant of Ly108 that lacks both exons 7 and 8

The detection of Ly108-H1 by R4 but not by R1, which was raised against a peptide sequence encoded by exon 7, suggested that the R1 peptide sequence, containing the second immuno-tyrosine switch motif (ITSM), was absent from Ly108-H1 (Fig. 3 D). Based on the protein analyses, we tested the possibility that lymphocytes from *Slamf*-haplotype 1 mice expressed an Ly108 splice variant lacking sequences for exons 7 and 8. Using exon 1– and exon 9–specific primer pairs, two PCR products, presumably Ly108-2 and Ly108-H1, were amplified from *B6* thymocytes (Fig. 3 A). Subsequent cloning and sequence analysis of the cDNAs confirmed that *B6* thymocytes indeed express a transcript that lacks both exons 7 and 8 (GenBank/EMBL/DDBJ accession no. ACF05482).

To determine whether this novel transcript encodes Ly108-H1, three cDNAs were transiently transfected into the Ly108-negative T cell line BI-141 (Fig. 3 B). Immunoprecipitation followed by deglycosylation with PNGaseF, SDS-PAGE, and immunoblotting verified that Ly108-Δ *exon 7/8* cDNA encoded the Ly108-H1 protein, as judged by its

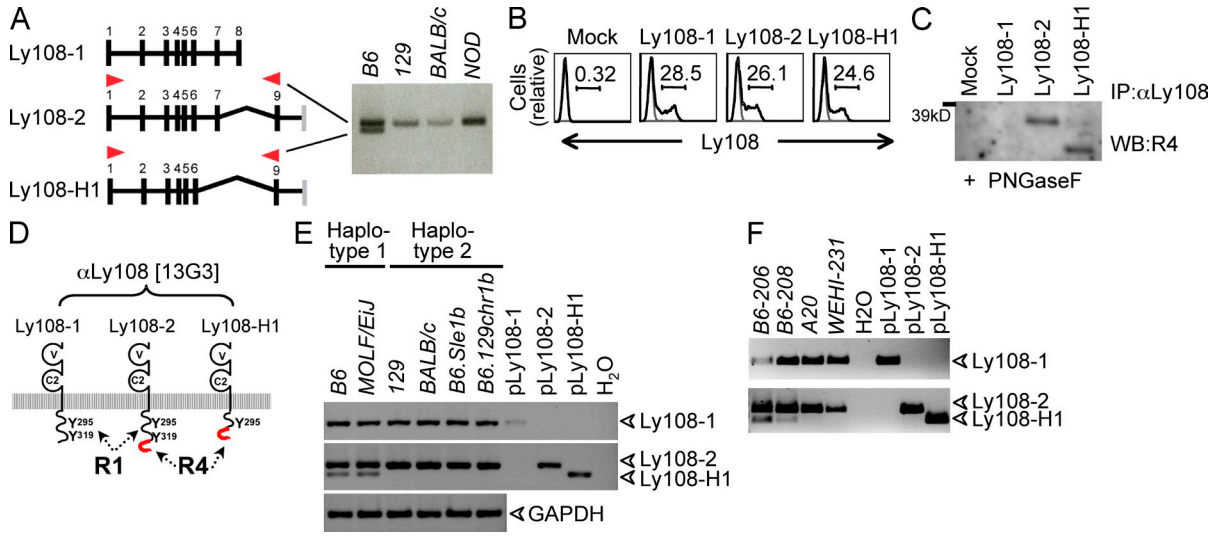

Figure 3. The Ly108-H1 protein is encoded by a splice variant of Ly108 that lacks both exons 7 and 8. (A, left) Diagram of the nine exons of the Ly108 gene. Both exons 8 and 9 contain a 3′ untranslated region. Location of the exon 1–9 primers is indicated with red arrowheads. (right) RT-PCR using mRNA from *B6*, *129*, *BALB/c*, and *NOD* thymocytes. (B) Ly108 cell surface expression on $CD4^+$ T hybridoma cells that were transiently transfected with cDNAs encoding Ly108-1, Ly108-2, or Ly108-H1. Surface expression was evaluated by flow cytometry 24 h after transfection. (C) Lysates of the Ly108-1, Ly108-2, or Ly108-H1 BI-141 transfectant cells were immunoprecipitated with α-Ly108, treated with PNGaseF, subjected to SDS-PAGE, and evaluated by Western blotting (WB) with the R4 polyclonal antibody. IP, immunoprecipitate. (D) Schematic illustration of the three Ly108 protein isoforms. Antibody R1 binds a segment shared by the isoforms Ly108-1 and Ly108-2. Antibody R4 is directed against the C-terminal amino acid sequence of isoforms Ly108-2 and Ly108-H1. (E) RT-PCR analyses of isoform mRNAs isolated from thymocytes of *Slamf*-haplotype 1 and 2 WT and congenic mouse strains. Primers specific for exons 5 and 8 recognize Ly108-1, and primers specific for exons 5 and 9 recognize Ly108-2 and Ly108-H1. Plasmids containing the cDNA sequences of individual isoforms (pLy108-1, pLy108-2, and pLy108-H1) were used as positive controls. (F) RT-PCR analyses of isoform mRNAs isolated from B cell lines. B6-206 and B6-208 are cloned B cell lymphoma lines derived from *B6* mice. WEHI-231 and A20 are derived from *BALB/c* mice (*Slamf*-haplotype 2). All T cell experiments were performed two times; the B cell analysis was performed once using two different cell lines from each of the haplotypes.

molecular weight and reactivity with R4 (Fig. 3 C). Collectively, these data clearly demonstrate that T and B lineage cells from haplotype 1 but not haplotype 2 mice express Ly108-H1, in addition to the Ly108-1 and Ly108-2 proteins (Fig. 3 D).

Next, expression of Ly108-H1 in T and B cells from the lupus-prone congenic strains *Sle1b* and *B6.129chr1b* and from various *Slamf*-haplotype 1 and 2 mice was examined by RT-PCR. To this end, oligonucleotide primers that either spanned exons 5–8 (detecting Ly108-1) or exons 5–9 (common to Ly108-2 and Ly108-H1) were used. Ly108-H1 was detectable in *Slamf*-haplotype 1 but not in any haplotype 2 thymocytes (Fig. 3 E). More importantly, Ly108-H1 is absent in the congenic mouse strains *Sle1b* and *B6.129chr1b*, suggesting that the presence of this novel protein isoform might affect the development of lupus.

To evaluate whether single cells express all three isoforms, we used B cell lymphoma cell lines from different origins. These experiments showed that the *B6*-derived lines B6-206 and B6-208 coexpressed transcripts for all three isoforms, whereas the *BALB/c*-derived A20 and (*BALB/c* × *NZB*)F1-derived WEHI-231 cells coexpressed only Ly108-1 and Ly108-2 (Fig. 3 F).

The data with *Sle1b* and *B6.129chr1b* lymphocytes suggest that the alternate splice form, Ly108-H1, might have been generated by regulatory elements within the short *129*-derived segment in these congenic mouse strains and perhaps by elements that are part of, or in proximity to, the Ly108 gene. To evaluate this, a *B6*-derived and a *129*-derived BAC clone were each transfected into Jurkat T cells. Both transfectant cells expressed Ly108-1 and Ly108-2, but only in transfectants generated with the *B6*-derived BAC clone could Ly108-H1 be detected (Fig. S3, A and B). Our sequence analyses indicated that the splice donor and acceptor sequences in the introns surrounding exons 6–8 are identical between *B6* and the congenic mouse strains *Sle1b* and *B6.129chr1b* (Fig. S3 C). However, two pyrimidine-rich tandem repeat sequences were only present in intron 6 of the *B6* mouse (Fig. S3 C), which could be the cause for the alternate splicing events that generate the protein isoform Ly108-H1 (Wagner and Garcia-Blanco, 2001; Black, 2003).

Collectively, these data clearly demonstrate that T and B lymphocytes from *Slamf*-haplotype 1 but not haplotype 2 mice coexpress the Ly108-1, Ly108-2, and Ly108-H1 protein isoforms. We conclude that Ly108-H1 is generated by elements within the *B6*-derived BAC clone, most likely by sequences in intron 6, which could negatively regulate splicing and which are absent in *Slamf*-haplotype 2 mice.

Faithful expression of an Ly108-H1 BAC-based transgene BACLy108-H1 in *Sle1b* mice

Because Ly108-H1 is not expressed in the congenic *Sle1b* and *B6.129chr1b* mice, we hypothesized that this isoform could have a protective role in murine lupus. To this end, we introduced the Ly108-H1 isoform into the *Sle1b* mouse. However, introduction of an Ly108-H1–specific transgene might be complicated by regulatory elements in and in proximity to the Ly108 gene and by the possibility of overexpressing the transgene in a tissue-biased manner. We therefore introduced into the *Sle1b* mouse a *B6*-derived BAC clone–based transgene, which only expressed Ly108-H1. This required several alterations of the BAC clone RP23-77A8 (Osoegawa et al., 2000). First, through recombineering in *Escherichia coli*, we removed a DNA fragment containing Ly108 exons 7 and 8, thus preventing potential expression of Ly108-1 and Ly108-2 by the transgene. Next, the genomic sequences encoding SLAM (*Slamf1*) and CD84 (*Slamf5*) were removed by two subsequent recombineering steps. Because the Ly108 amino acid sequence does not differ between haplotype 1 and haplotype 2 strains, the transgene simply reconstructed a missing splicing event in the transcriptome of *Sle1b* mice. The resulting ∼100-kb genomic BACLy108-H1 vector should only contain the genomic cis-sequences that are requisite for faithful transcription of only the Ly108-H1 isoform (Fig. 4 A).

Transgenesis of the BACLy108-H1 vector into *Sle1b* mice resulted in the *Sle1b*.BACLy108-H1 mouse with the transgene located in one area of the genome, as judged by fluorescent in situ hybridization (Fig. S4 A). Semiquantitative RT-PCR indicated that Ly108-H1 was expressed in thymocytes derived from hemizygous transgenic *Sle1b*.BACLy108-H1 mouse, while absent in *Sle1b* thymocytes (Fig. 4 B). To further evaluate the faithful transcription of all three of the Ly108 isoforms, we took advantage of the fact that Ly108 transcripts originating from *B6* and *Sle1b* differ from each other in several synonymous SNPs (NCBI mouse SNP database). Indeed, the *Sle1b*.BACLy108-H1 mice express exons 2–4 both of *Slamf*-haplotype 1 (encoded by BACLy108-H1) and of *Slamf*-haplotype 2 (encoded by *Sle1b*; Fig. 4 C). Examination of the RFLPs of thymocyte-derived Ly108 cDNA confirmed that Ly108-1/2 expression in *Sle1b*.BACLy108-H1 thymocytes was controlled by the *Slamf*-haplotype 2 segment of the *Sle1b* mouse (Fig. 4 D, left). The BAC transgene did not express SLAM and CD84, as judged by the use of two different SNP-based RFLPs (Fig. 4 D, middle and right).

Cytofluorimetric analyses of Ly108 expression on the surface of T lineage cells isolated from *Sle1b*, *Sle1b*.BACLy108-H1, or *B6* mice (Fig. 4 E) supported the notion that Ly108 surface expression on T cells was slightly higher in hemizygous *Sle1b*.BACLy108-H1 mice than their *Sle1b* transgene-negative littermates. And, as expected for mice that are hemizygous for the Ly108-H1 transgene and homozygous for the *Slamf*-haplotype 2 forms of Ly108, surface expression was not as high as on the surface of *Slamf*-haplotype 1, e.g., *B6* thymocytes (Figs. 2 and 4 E). The overall T and B lymphocyte development was normal in young *Sle1b*.BACLy108-H1 mice (Fig. S4 B). Collectively, these results indicate that, at most, one copy of Ly108-H1 was expressed in *Sle1b*.BACLy108-H1–derived T lineage cells and that cell surface expression and balance between the three isoforms was similar to that found in the *B6* mouse.

The presence of the Ly108-H1 isoform in *Sle1b* mice ameliorates the development of lupus-related autoimmunity

To assess whether Ly108-H1 would affect the spontaneous development of SLE in *Sle1b* mice, we analyzed a cohort

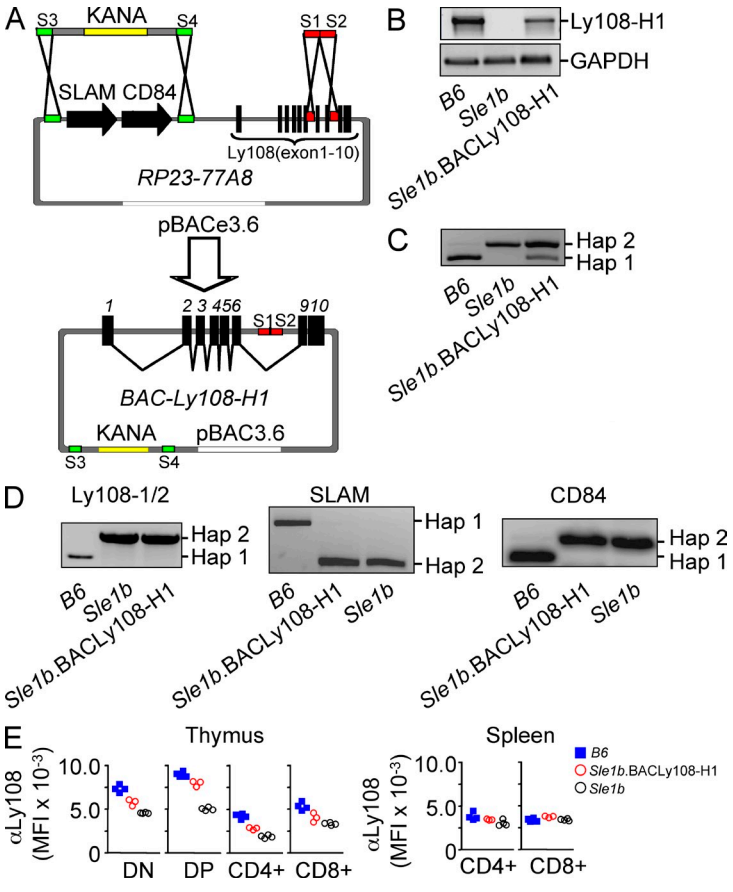

Figure 4. Expression of an Ly108-H1 BAC-based transgene in *Sle1b* mice. (A) The BACLy108-H1 transgene vector encoding Ly108-H1 was generated by deleting exons 7 and 8 of Ly108 and the SLAM and CD84 genes from the *B6* BAC clone RP23-77A8. Alteration of the 200-kb *B6* BAC clone by Red/ET recombineering is described in Materials and methods. The resulting DNA fragment BACLy108-H1 is ∼100 kb. S1, S2, S3, and S4 are homology arms for Red/ET recombination. KANA is a kanamycin resistance gene cassette. (B) RT-PCR prepared with thymic mRNA using Ly108-H1–specific primers. (C) Haplotype (Hap)-specific RFLP fragments were obtained by BsrI digestion of PCR-amplified thymic Ly108 cDNA. *B6* and *Sle1b* mice exclusively express haplotype 1– and haplotype 2–specific fragments, respectively. Because *Sle1b*.BACLy108-H1 mice express both fragments, the transgene expresses the *B6* based fragment. PCR primer pairs specific for Ly108 exons 2–4 (common for Ly108-1, Ly108-2, and Ly108-H1) were used, as described in Materials and methods. (D, left) RT-PCR primers specific for Ly108 exons 2–7 (common for Ly108-1 and Ly108-2 only) were used to isolate a cDNA from the thymus. Haplotype 1– and haplotype 2–specific RFLP used BsrI digestion, as in C. (middle) RT-PCR primers specific for SLAM exons 1–5 were used to isolate a cDNA from the thymus. Haplotype 1– and haplotype 2–specific RFLP fragments were obtained by TaqI digestion. (right) RT-PCR primers specific for CD84 exons 1–2 were used to isolate cDNA. Haplotype-specific RFLP fragments were obtained by MspI digestion. (E) Cell surface expression of Ly108 using T lineage cells isolated from *Sle1b*, *Sle1b*.BACLy108-H1, or *B6* mice. Thymic and splenic T cells were incubated with the monoclonal α-Ly108 antibody (13G3) conjugated with DyLight 649 and then washed and analyzed by flow cytometry. The mean fluorescent intensity (MFI) of gated cell populations in the DyLight 649 channel is shown (three to four individual mice per group). PCR experiments were performed a minimum of two times. DN, double negative; DP, double positive.

of aged female hemizygous *Sle1b*.BACLy108-H1 mice and transgene-negative *Sle1b* littermate controls along with *B6* females. Whereas the *Sle1b* mice (6–8 mo old) had high titers of antinuclear antibodies (ANAs), as judged in a HEp-2 cell–based fluorescence quantitative assay, spontaneous development of these autoantibodies was significantly lower in their transgenic littermates (Fig. 5 A). Similarly, antinucleosome IgG and antichromatin IgG titers were dramatically lower in *Sle1b*.BACLy108-H1 as compared with the *Sle1b* mice (Fig. 5, B and C).

The presence of the Ly108-H1 transgene in aged *Sle1b* mice affected the activation of T and B cells (Table S1). First, in aged *Sle1b* mice, a significant increase in activated $CD69^+$ and $CD44^+CD62L^-$ effector/memory $CD4^+$ T cells was found compared with *B6* mice. This effect was strongly reduced by the presence of the Ly108-H1 transgene (Fig. 5 D and Table S1). To exclude transgene integration site–dependent artifacts, we also demonstrated this phenotype in a second independently derived BACLy108-H1 transgenic founder line (Fig. S4, C–E). Similarly, the percentage of IFN-γ–expressing $CD4^+$ cells was lower in aged *Sle1b*.BACLy108-H1 mice than in *Sle1b* mice. The spontaneous expansion of germinal center B cells and contraction of the marginal zone B cells in *Sle1b* mice was substantially reversed by Ly108-H1 (Fig. 5 E and Table S1).

We conclude that the presence of Ly108-H1 partially suppresses the key humoral autoimmune features of *Sle1b* mice, i.e., autoantibody production, spontaneous activation of peripheral T cells, and expansion of germinal center B cells. This is remarkable because the DNA segment derived from *NZW*, i.e., *Slamf*-haplotype 2, contains 7 *Slamf* genes and >12 other genes, which might somehow contribute to *Sle1b*-based lupus (Wandstrat et al., 2004; Calpe et al., 2008).

Ly108-H1 in $CD4^+$ T cells ameliorates autoimmunity in a transfer model of SLE

Whereas previous studies indicate that a defect in early B cell development is a major contributor to lupus in the *Sle1b* mouse (Kumar et al., 2006; Chang et al., 2009), a role for peripheral T cells cannot be excluded in this congenic mouse. We therefore directly tested the possibility that *Sle1b* $CD4^+$ T cells could induce autoantibody production in an established transfer model of SLE (Morris et al., 1990). As shown in Fig. 6 A, the transfer of *Sle1b* splenocytes into *bm12* recipients induces much higher anti–double-stranded DNA (dsDNA) IgG titers than the transfer of splenocytes derived from WT *B6* mice, particularly at 4 wk after transfer. Second, both purified *Sle1b* $CD4^+$ T cells or $CD62L^+$ naive $CD4^+$ T cells (Fig. 6 B and Fig. S5, A–E) consistently induced stronger

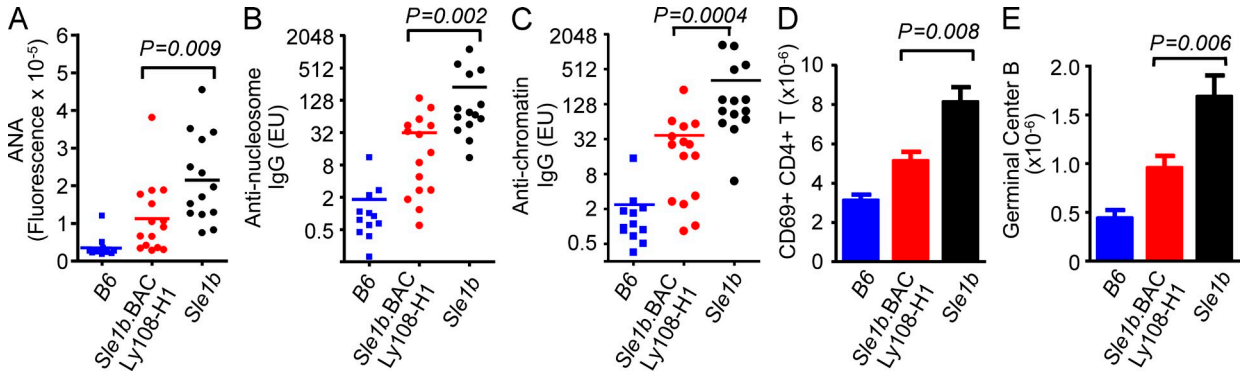

Figure 5. The presence of the Ly108-H1 isoform in *Sle1b* mice ameliorates spontaneous development of SLE. All experiments in this figure were performed using sera (A–C) or splenocytes (D and E) from one cohort of 6–8-mo-old female mice: *B6*, *n* = 12; *Sle1b*, *n* = 14; *Sle1b*.BACLy108-H1, *n* = 15. (A) Comparison of ANA titers in aged *Sle1b*, *Sle1b*.BACLy108-H1, and *B6* mice. Monolayers of permeabilized HEp-2 cells were incubated with sera from 6–8-mo-old female mice. The cells were washed, and bound IgG was detected with anti-mouse IgG–Alexa Fluor 488 and quantitated by fluorescent microscopy (see Materials and methods). Statistical analyses were performed as in Fig. 1. (B) Antinucleosome antibody titers in sera of 6–8-mo-old female *Sle1b*, *Sle1b*.BACLy108-H1, and *B6* mice was detected by ELISA (see Materials and methods). (C) Antichromatin antibody titers were detected as in B. (A–C) The mean titer is indicated by a horizontal bar. EU, ELISA units. (D) Number of $CD69^+CD4^+$ activated T cells in the spleen of aged *Sle1b*.BACLy108-H1 and *Sle1b* mice. Staining and flow cytometry were performed as described in Materials and methods. (E) Number of germinal center B cells ($GL7^{hi}$ Fas^{hi} $B220^+$) in the spleen of aged *Sle1b*.BACLy108-H1 and *Sle1b* mice. Staining and flow cytometry were performed as described in Materials and methods. (D and E) Error bars indicate SEM of samples from 12–15 animals per group.

autoantibody responses when transferred into *bm12* mice than the transfer of the same cells isolated from WT *B6* mice. This result strongly supported a role for peripheral $CD4^+$ T cells in the spontaneous *Sle1b* disease.

A comparison of autoantibody responses to the transfer of cells derived from *Sle1b* or *Sle1b*.BACLy108-H1 mice into *bm12* recipients showed that Ly108-H1–expressing splenocytes or $CD4^+$ T cells ameliorate autoreactive responses (Fig. 6, C and D; and Fig. S5, D and E). Furthermore, transferring *Sle1b*.BACLy108-H1 splenocytes or $CD4^+$ T cells into *bm12* recipients induces less $CD4^+$ T cell activation (Fig. 6 E) than transfer of *Sle1b*-derived cells. Similarly, less B cell activation is found upon transfer of *Sle1b*.BACLy108-H1 cells compared with *Sle1b* cells (Fig. S5 F).

An in vitro experiment confirmed the notion that Ly108-H1 affects T cell proliferation when naive $CD4^+$ T cells isolated from *Sle1b*, *Sle1b*.BACLy108-H1, and *B6* mice were stimulated with limiting amounts of α-CD3. Under the conditions used, *Sle1b* $CD4^+$ T cells responded with a robust proliferation (Fig. 6 F), suggesting that they are indeed intrinsically prone to undesirable immune activation. However, as predicted by our in vivo observations (Fig. 6 D and Fig. S5 E), this phenotype of naive $CD4^+$ *Sle1b* T cells was dramatically reduced in naive *Sle1b*.BACLy108-H1 $CD4^+$ T cells (Fig. 6 F). Similar results were obtained with measuring proliferation by CFSE dilution (Fig. S5 G).

Collectively, the outcomes of this set of experiments demonstrate that, in contrast to previous suggestions that Ly108 controls T and B cell development (Kumar et al., 2006; Kanta and Mohan, 2009), peripheral *Sle1b* $CD4^+$ T cells play a major role in the pathogenesis of SLE. More importantly, the transfer of Ly108-H1–expressing *Sle1b* T cells causes significantly less disease than the transfer of the same number of *Sle1b* T cells. We conclude that a balanced expression of the Ly108-H1 isoform in $CD4^+$ T cells ameliorates SLE in *Sle1b* mice and may dampen in vivo and in vitro T cell activations.

DISCUSSION

In mice, genome-wide linkage studies have implicated the syntenic region to human 1q23 in three different models of spontaneous lupus: the (*NZB* × *NZW*)F2 intercross, the NZM/Aeg2410 New Zealand mice, and the BXSB mice (Kono et al., 1994; Rozzo et al., 1996; Hogarth et al., 1998). The phenotype of these mice is very similar to that in SLE patients, with the production of autoantibodies, as well as multiorgan involvement, including severe nephritis. In congenic mice derived from the NZM2410 mouse strain and *B6*, the locus on chromosome 1, i.e., *Sle1*, by itself was sufficient to generate a strong, spontaneous, humoral ANA response. *Sle1* also led to an expanded pool of histone-reactive T cells. Thus, *Sle1* may lead to the presentation of chromatin in an immunogenic fashion or directly impact tolerance of chromatin-specific B cells. Consequently, *Sle1* is thought to be a major player in orchestrating selective loss of B cell and T cell tolerance to chromatin. Fine mapping of the *Sle1* locus determined that three loci within this congenic interval, termed *Sle1a*, *Sle1b*, and *Sle1c* (Morel et al., 2001), could independently cause a loss of tolerance to chromatin, which is a necessary step for full disease induction. The *Sle1b* region, an ∼0.9-Mb *Slamf*-haplotype 2–derived, i.e., *NZW*-derived, DNA segment which includes the *Slamf* locus, was implicated as a major contributor to the role of *Sle1b* in tolerance (Wandstrat et al., 2004).

Similar to the *Sle1b* mouse, *B6.129chr1b* mice also develop lupus (Bygrave et al., 2004; Carlucci et al., 2007). In these mice, the *Slamf* genes are derived from the *129*

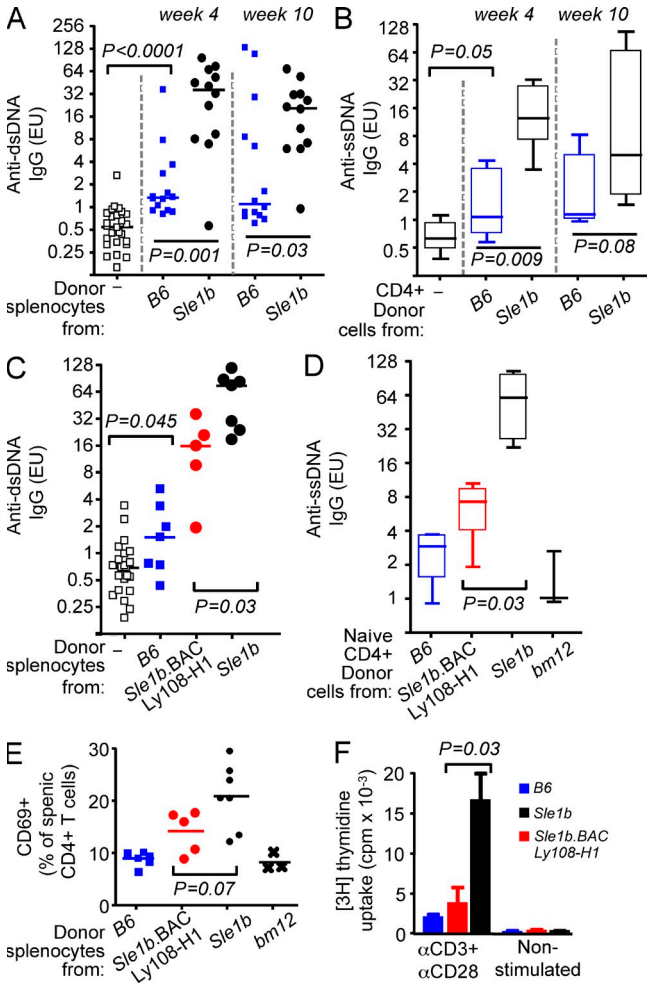

Figure 6. The presence of Ly108-H1 in *Sle1b* CD4⁺ T cells ameliorates SLE in a transfer model of SLE. (A) 5×10^7 splenocytes isolated from individual *B6* or *Sle1b* mice were transferred into *bm12* recipients by i.p. injection. After 4 or 10 wk, anti-dsDNA antibodies in the serum were determined by ELISA and are expressed as ELISA units (EU). *B6* → *bm12*, $n = 14$; *Sle1b* → *bm12*, $n = 12$. Data points shown are pooled from two experiments. (B) 7×10^6 CD4⁺ T cells isolated from *B6* or *Sle1b* mice were transferred into *bm12* recipients by i.p. injection. After 4 or 10 wk, anti-ssDNA antibodies in the serum were determined by ELISA and were expressed as ELISA units. *B6* → *bm12*, $n = 5$; *Sle1b* → *bm12*, $n = 6$. (A and B) Statistical analyses were performed as in Fig. 1. Median values are indicated by a horizontal line. (C) 5×10^7 Splenocytes isolated from individual donors were transferred into *bm12* recipients by i.p. injection. After 4 wk, anti-dsDNA IgG autoantibodies were determined. *B6* → *bm12*, $n = 7$; *Sle1b*.BACLy108-H1 → *bm12*, $n = 5$; *Sle1b* → *bm12*, $n = 7$. (D) 2.5×10^6 naive (CD62L⁺) CD4⁺ T cells isolated from the spleen of *B6*, *Sle1b*, or *Sle1b*.BACLy108-H1 mice were transferred into *bm12* recipients by i.p. injection. After 4 wk, anti-ssDNA antibodies in the serum were determined by ELISA and are expressed as ELISA units. *B6* → *bm12*, $n = 5$; *Sle1b*.BACLy108-H1 → *bm12*, $n = 4$; *Sle1b* → *bm12*, $n = 4$; *bm12* → *bm12*, $n = 3$. (C and D) Statistical analyses were performed as in Fig. 1. (E) CD4⁺ T cell activation upon transfer of *B6*, *Sle1b*.BACLy108-H1, and *Sle1b* splenocytes into *bm12* recipients. See C. (F) Naive CD4⁺ T cells isolated from the spleen of the indicated mice were activated with a suboptimal dose of anti-CD3 and anti-CD28. Proliferation was determined by pulsing with [³H]thymidine on day 2 and harvesting 16 h later. Mean and SEM of three samples (10^5 cells/well) generated from the pool of two animals. The result is representative of two independent experiments (statistical analysis by two-tailed unpaired *t* test).

nonautoimmune genetic background, supporting the theory that autoimmunity occurs because of unidentified epistatic genetic interactions between the haplotype 2 *Slamf* locus and the *B6* background genes (Morel et al., 1999; Bygrave et al., 2004; Wandstrat et al., 2004; Carlucci et al., 2010). The experiments in this paper set out to demonstrate that elimination in the congenic mouse Ly108$^{-/-}$ [*129* × *B6*] of both Ly108-1 and Ly108-2 leads to an absence of disease when compared with the control mouse Ly108⁺ *B6.129chr1b*. Surprisingly, protein analyses identified the novel *Slamf*-haplotype 1–specific isoform Ly108-H1, which has only one of the two ITSMs that binds the SH2 domain adapter SLAM-associated protein (SAP) in T and NK cells. The mechanism, which leads to this alternative splice form being expressed exclusively in *Slamf*-haplotype 1 mice, is located within the Ly108 gene itself. First, the observation that Ly108-H1 is not expressed in *Sle1b*, which is a *B6* mouse with an ∼0.9-Mb insert derived from the *Slamf*-haplotype 2 mouse *NZW* (Wandstrat et al., 2004), suggests that this small genomic inset is endowed with the capability to control this particular alternative splicing event. Second, several DNA sequences, which could influence local splicing, are present in intron 6 of *B6* but not in the *Slamf*-haplotype 2 mice. Third, Jurkat cells transfected with the Ly108 containing *B6*-derived BAC clone (RP23-77A8) express Ly108-H1 messenger RNA (mRNA), which is not detectable in Jurkat cells transfected with the *129*-derived BAC clone (bMQ241k20).

Several recent studies support a model in which T cells isolated from SLE patients surprisingly express protein isoforms that are infrequently found in cells from healthy individuals. For instance, unusual CD3-ζ and CD44 isoform mRNAs have been found in lupus patients, which lead to mutant CD3-ζ proteins that alter TCR/CD3 signaling (Nambiar et al., 2001; Tsuzaka et al., 2003; Crispín et al., 2010a). Similarly, some isoforms of the *IRF5* gene, which is genetically associated with lupus (genome-wide association study SNP), are highly expressed in patients but not in healthy individuals (Graham et al., 2006). Furthermore, only the short isoform of CD244 (SLAMF4), which is an alternative splicing product, was associated with lupus (Kim et al., 2010). How the alternate splice forms of mouse Ly108-1 and Ly108-2 are generated is not known in detail, but the presence of two 3′ untranslated region sequences in all healthy mice suggests that the decision process might be stochastic (Fig. S3 B). Although the presence or absence of Ly108-H1 protein marks the major difference between Ly108 in *Sle1b* and *B6* mice, we cannot exclude the idea that subtle differences in expression of Ly108-1 and Ly108-2 contribute to cooperation between the three isoforms in a given cell. In addition to the two well characterized isoforms, Zhong and Veillette (2008) recently

reported a rare transcript termed Ly108-3. This isoform, when ligated, mediates a tyrosine phosphorylation signal that is intermediate between Ly108-1 and Ly108-2. This protein isoform could not be detected in our experiments.

Transgenesis of the BACLy108-H1 vector encoding Ly108-H1 into *Sle1b* mice had a dramatic effect on the spontaneous development of lupus. Remarkably, expression of Ly108-H1 significantly decreased autoantibody titers, percentages of spontaneously activated T and B cells in the spleen, and expansion of germinal center B cells in aged *Sle1b*.BACLy108-H1 mice compared with their *Sle1b* littermate controls. Despite not completely reversing the autoreactive phenotype normally observed in *Sle1b* mice, our results indicate that Ly108-H1 is a major player in regulating Ly108-mediated autoimmunity. This lack of a full phenotype reversal can be explained in part by our semiquantitative PCR data, which suggest that Ly108-H1 is expressed at lower levels in the hemizygous transgenic animals than in the *B6* mouse (Fig. 4 B). Moreover, in *Sle1b* mice, the putative pathogenic isoform, Ly108-1, has an elevated expression level compared with the *B6* mouse (Wandstrat et al., 2004), which might be difficult to overcome by inhibitory signals.

Although activation of both T and B cells was affected by the presence of Ly108-H1, we focused on the role of peripheral $CD4^+$ T cells in transfer experiments. Although T cells in the *Sle1* congenic mice show a broad range of autoimmune phenotypes (e.g., spontaneous $CD4^+$ T cell activation, decreased number of T regulatory cells, presence of histone-specific T cells, and increased proliferation and cytokine production; Morel et al., 2001; Chen et al., 2005), the *Sle1b* subcongenic mice carry only a fraction of these defects (i.e., increased percentage of activated T cells and elevated calcium influx after receptor cross-linking [Wandstrat et al., 2004; Chen et al., 2005]). In this study, we show that the transfer of peripheral $CD4^+$ cells derived from *Sle1b* mice into *bm12* recipients induces T and B cell activation and autoantibody responses that are much more robust than after the transfer of *B6* cells, work that directly links, for the first time, T cell–intrinsic phenotypes of *Sle1b* with lupus development. The transfer of *Sle1b* cells expressing Ly108-H1 results in a much lesser autoantibody and T cell responses compared with the responses to *Sle1b* cells. This ameliorating effect of Ly108-H1 is caused by a mechanism that results in dampening in vivo and in vitro T cell proliferation and not by reduced activation-induced cell death.

Recently, experiments with *Sle1b*-derived B cells led to the conclusion that Ly108-2, in contrast to Ly108-1, is able to sensitize immature B cells to deletion (Kumar et al., 2006). Preliminary transfections in WEHI-231 cells (unpublished data) suggest that in contrast to Ly108-2, Ly108-H1 does not affect apoptosis. In the model in Fig. 7, we therefore hypothesize that Ly108-1 is a pathogenic allele that operates in immature B cells and peripheral T cells. Ly108-2 and the novel isoform Ly108-H1 are both associated with disease protection: whereas Ly108-2 contributes to sensitizing T and B cells to apoptosis, Ly108-H1 is an effective suppressor of pathogenic T cell proliferation in *Sle1b*. Based on these functional differences between the Ly108 isoforms, it is likely that Ly108-H1 mediates distinct inhibitory signaling events rather than passively interfering with signals initiated by Ly108-1 and Ly108-2. This hypothesis is supported by the observation that the BACLy108-H1 transgene only causes a small increase in total Ly108 surface expression on peripheral $CD4^+$ T cells, making it improbable that Ly108-H1 is affecting clustering of the other Ly108 molecules in the immunosynapse. Additionally, expression of the Ly108-H1 transgene dampens proliferation in $CD4^+$ T cells, whereas $Ly108^{-/-}$ mice maintain normal levels of proliferation (Howie et al., 2005; unpublished data generated with *B6*.$Ly108^{-/-}$), further supporting the notion that Ly108-H1 is an active signaling molecule. As yeast two-hybrid screenings have identified that both ITSMs, associated with the Y^{295} and Y^{319} of Ly108, are capable of binding SAP (Fraser et al., 2002), it is likely that Ly108-H1, which also contains one of these motifs, is also capable of recruiting the adapter protein SAP. Additionally, as Ly108 was recently shown to participate in stabilizing T cell–B cell conjugate formation in a SAP-binding dependent manner (Cannons et al., 2010), dissecting the role of Ly108 isoforms in cell–cell networking processes that govern autoantibody production could be an exciting area for further investigations. As an interest in gene isoform–dependent mechanisms is rapidly increasing and because isoform expression appears to be altered in lupus patients, the outcomes of our experiments relate to a larger concept that an interplay between isoforms provides for a plethora of regulatory possibilities in developmental biology, as well as in pathogenesis of diseases.

MATERIALS AND METHODS

Mice. *B6*, *NOD*/LtJ, *MOLF/EiJ*, *BALB/c*, and *B6*.C-H-2bm12/KhEg (*bm12*) mice were obtained from the Jackson Laboratory. *129*/SvEvTac (*129*) mice were obtained from Taconic. *B6.129chr1b* (Carlucci et al., 2007) mice were donated by M. Botto (Imperial College London, London, England, UK). *B6.Sle1b* (*Sle1b*; Morel et al., 2001) mice were provided by L. Morel (University of Florida, Gainesville, FL). $Ly108^{-/-}$ [*129* × *B6*] (Howie et al., 2005) was backcrossed six times with *B6*, and breeders were selected for the smallest congenic interval. Animal experiments were approved by the Beth Israel Deaconess Medical Center Institutional Animal Care and Use Committee.

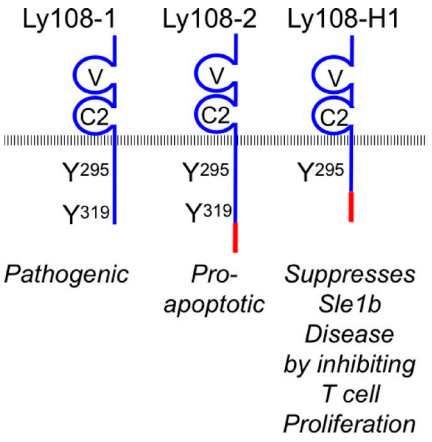

Figure 7. Schematic outline of the proposed role of the Ly108 protein isoforms in the pathogenesis of disease in *Sle1b* mice.

Genotypic analysis. Genomic DNA of Ly108$^{-/-}$ [*129* × *B6*] and *B6.129chr1b* mice was analyzed with polymorphic genetic markers. PCR was performed using 10 markers on chromosome 1 and at least 1 marker per other chromosomes. Primer sequences were obtained from the Mouse Genome Informatics database. Fine mapping of congenic boundaries was performed by the Jackson Laboratory (JAX Mouse Diversity Genotyping Array Service). In brief, mouse genomic DNA was labeled and hybridized on a custom Affymetrix array. The mean resolution of the analysis was one SNP every 4.3 kb.

Generating the *Sle1b*.BACLy108-H1 mice. RP23-77A8 BAC clone, containing full-length *B6* Ly108, CD84, and SLAM, was obtained from the BACPAC Resources Center at Children's Hospital Oakland Research Institute. Exons 7–8 and the surrounding intronic region of the Ly108 gene were removed by Red/ET recombination (Muyrers et al., 1999) using a commercial kit (Gene Bridges GmbH) according to the manufacturer's protocol. In brief, S1 (5′-TAAAGGAGCAAGCCTGGAATCAGATGCAAGACAAGAATGCTTTTATCCCT-3′) and S2 (5′-AATACACAGAAGTAGACCTACAGTTGCAGAGCCAATCATATTGTTTCATT-3′) homology arms were used to target a 2.8-kb fragment containing Ly108 exons 7 and 8 and replacing it with a single PmeI site. To remove a 130-kb genomic region containing SLAM and CD84, we performed a second recombination step using S3 (5′-AGGTCATCCTCTATCCTAACCTCAGAGAAGCACTTCCTGCACATCACTAG-3′) and S4 (5′-GTTATGGACATGATCTGCATTCATGTTCATGGGCATTTAGGATTTCACTG-3′) homology arms. Vector was injected into *Sle1b* oocytes by the Beth Israel Deaconess Transgenic Core Facility. Screening of founders was performed by PCR.

Murine transfer model of lupus. As described by Morris et al. (1990), 7–9-wk-old naive female *bm12* mice were injected i.p. with splenocytes, purified CD4$^+$ T cells, or purified CD62L$^+$ CD4$^+$ naive T cells (magnetic bead cell separation; Miltenyi Biotec) from age- and sex-matched donors.

RT-PCR. RNA was isolated from cells using the RNeasy kit (QIAGEN) or TRIZOL (Invitrogen). RT was performed with the Protoscript cDNA kit (New England Biolabs, Inc.). A full-length RT-PCR was performed on cDNA templates with the following primers with introduction of restriction sites: 5′ XhoI-Ly108-1/2/H1 start, 5′-GGCTCGAGATGGCTGTCTCAAGGGCT-3′; 3′ Ly108-1 end XbaI, 5′-GGTCTAGATTAAGAGTATTCGGCCTCTCTGG-3′; and 3′ Ly108-2/H1 end XbaI, 5′-GGTCTAGATCAGGAGTTATAGTTGATTAAAGTGTT-3′.

A shorter PCR was performed for better separation of the isoforms with the following primers: 5′ (in exon 5), 5′-TTTGACTAGCCAACATCC-3′; 3′ Ly108-1, 5′-TTAAGAGTATTCGGCCTC-3′; and 3′ Ly108-2/H1, 5′-TCAGGAGTTATAGTTGAT-3′. RT-PCR for selective amplification of Ly108-H1 was performed with the primers Ly108-H1 forward, 5′-CCTACTCCCTGCAAATCAGC-3′; and Ly108-H1 reverse, 5′-CCGGTTAAAGCCACTGTTTCCTG-3′. GAPDH-specific primers were obtained from New England Biolabs, Inc.

Haplotype-specific RT-PCR and RFLP. For RFLP assays, polymorphic Ly108, SLAM, and CD84 cDNA fragments were amplified by PCR. All amplified fragments contained haplotype-specific SNPs (NCBI dbSNP or Mouse Genome Informatics databases) with allele-selective restriction digestibility. Digested PCR products were analyzed by agarose gel electrophoresis.

The following primers were used with the corresponding restriction enzymes (New England Biolabs, Inc.): Ly108 all isoform (NCBI SNP accession no. rs31528124) primers: forward, 5′-CCTACTCCCTGCAAATCAGC-3′; and reverse, 5′-GCTCCAGCACACAAAGATGA-3′ digested with BsrI; Ly108-1 and Ly108-2 isoform (NCBI SNP accession no. rs31528124) primers: forward, 5′-CCTACTCCCTGCAAATCAGC-3′; and reverse, 5′-TGGAGTAAATTGTCATGGAGTCA-3′ digested with BsrI; SLAM all isoform (NCBI SNP accession no. rs31531636) primers: forward, 5′-GCTTCTTCCTTGGGGGTAAC-3′; and reverse 5′-TTTTTCTTCCACTGGTGGCT-3′ digested with TaqI; and CD84 all isoform (NCBI SNP accession no. rs31528577) primers: forward, 5′-ATGGCCCAGCGCCATCTGTGGATC-3′; and reverse 5′-TCTTGGTGATGGTTTCCTCA-3′ digested with MspI.

Generation of monoclonal antibodies directed against murine Ly108. Monoclonal antibodies directed against Ly108 were generated by immunizing an Ly108-deficient mouse (Howie et al., 2005) with WT thymocytes. Splenocytes were fused with NS1 myeloma cells and selected according to standard protocols. After three rounds of subcloning, the clone 13G3 (IgG2a) was selected based on reactivity with Ly108-Fc, as judged by ELISA.

Polyclonal antibodies. Antisera R1 and R4 directed at the cytoplasmic tails of Ly108 isoforms were generated by immunizing female New Zealand white rabbits with peptides conjugated via the N-terminal cysteine to KLH (Thermo Fisher Scientific). Antiserum R1, which recognizes both Ly108-1 and Ly108-2, was generated against the peptide Cys-KNDSMTIYSIVNHSRE. Antiserum R4, recognizing Ly108-2 and Ly108-H1, was directed against the peptide Cys-ALTGYNQPITLKVNTLINYNS.

Immunoprecipitation and Western blotting. Ly108 was precipitated from cell lysates with α-Ly108 (13G3) and protein G agarose (Invitrogen). Purified proteins were resolubilized before deglycosylation at 37°C for 2 h with immobilized carbohydrate binding domain–PNGaseF fusion protein (CBM-PNGaseF), donated by A. Warren (University of British Columbia, Vancouver, British Columbia, Canada). Isoforms were separated on a 12% continuous SDS-PAGE gel with MOPS (morpholino propane sulfonic acid) running buffer (Invitrogen). After transfer to polyvinylidene fluoride membrane, Western blotting was performed with the indicated rabbit primary and anti–rabbit, light chain–specific secondary horseradish peroxidase–conjugated antibody (Jackson ImmunoResearch Laboratories, Inc.). Reactivity was detected by chemiluminescence with SuperSignal (Thermo Fisher Scientific).

Expression vectors. Ly108 isoforms were amplified by PCR with primers introducing XhoI and XbaI restriction sites and cloned into pCR2.1-TOPO (Invitrogen) before subcloning into the mammalian expression vector PCI-neo (Promega). Ly108-1 and Ly108-2 cDNAs were provided by E. Ruley (Vanderbilt University School of Medicine, Nashville, TN; Peck and Ruley, 2000). Ly108-H1 was amplified from *B6* thymus cDNA.

Cell transfection. Ly108 isoforms were transfected into 1–2 × 10^7 cells by electroporation (250 V and 960 μF) with 10 μg plasmid DNA in 400 μl OptiMEM (Invitrogen) using a cuvette with a 4-mm electrode gap (Bio-Rad Laboratories) and analyzed 24 h later.

Flow cytometry. Single cell suspensions of spleens and thymuses were stained with the following antibodies after blocking nonspecific binding with CD16/32 (93) and 20% rabbit serum or 10% rabbit serum, respectively: α-CD3 (17A2), α-CD4 (L3T4), α–CD8-α (53–6.7), α-CD19 (1D3), α-CD21 (eBio4E3), α-CD23 (B3B4), α-CD44 (IM7), α-CD62L (MEL-14), α-CD69 (H1.2F3), α-CD86 (GL-1), α-CD138 (281–2), α-B220 (RA3-6B2), α-Fas (Jo2), α-GL7 (GL-7), α–TCR-β (H57-597) purchased from eBioscience, BD, or BioLegend. PBS57-loaded CD1d tetramer was provided by the National Institutes of Health tetramer facility. When surface Ly108 staining was performed, we used Cy5- or DyLight 649–conjugated anti-Ly108 (13G3) or IgG2a isotype control. Data were acquired with a cytometer (LSRII; BD) and analyzed using FlowJo software (Tree Star). Dead cells were excluded upon DAPI uptake. For intracellular staining, we used IFN-γ (XMG1.2) and IL-2 (JES6-5H4) antibodies (from BioLegend and BD, respectively) after 5-h PMA (50 ng/ml) and ionomycin (1 μg/ml) activation and cell permeabilization (BioLegend kit). When aged mice from a cohort were analyzed on different days (Fig. 1 B), each flow cytometry assay included at least one age-matched WT control.

ELISA. Titer of antinucleosome (antihistone–DNA complex) antibodies in mouse sera were determined by ELISA as described previously (Mohan et al., 1998). In brief, met-BSA–precoated Immunolon (Dynatech) plates were

coated overnight with dsDNA and then with total histone solutions (Sigma-Aldrich). Samples were incubated on plates in various dilutions between 1:600 and 1:1,200, and then plates were washed, and autoantibodies were detected with anti–mouse IgG-HRPO (GE Healthcare).

Autoantibody titer was expressed as ELISA units, comparing OD values of samples with a standard curve prepared with serial dilutions of ANA-positive NZM2410 serum pool. Antichromatin and anti-dsDNA titers were determined as for the antinucleosome levels, except for the preparation of ELISA plates. UV-irradiated Immunolon plates were incubated overnight with 3 µg/ml chicken chromatin (Cohen and Maldonado, 2003) or mung bean nuclease (New England Biolabs, Inc.)–treated dsDNA (Sigma-Aldrich). Anti–single-stranded DNA (ssDNA) was determined as described previously (Walter et al., 2010).

ANA. Specificity of autoantibodies was determined by indirect immunofluorescence using permeabilized HEp-2 cells (Antibodies Inc.). After incubation with various dilutions of mouse sera, HEp-2 slides were developed with anti–mouse IgG F(ab′)2 (Invitrogen). Quantitative analysis was performed by acquiring fluorescent images (AxioImager M1; Carl Zeiss) and determining main fluorescent intensity of HEp-2 nuclei (Volocity; PerkinElmer).

T cell proliferation assay. Splenic naive $CD62L^+$ $CD4^+$ T cells were purified using magnetic cell purification (Miltenyi Biotec) and activated by 0.3 µg/ml plate-bound anti-CD3 (145-2C11) and 1 µg/ml anti-CD28 (37.51) for 3 d on 96-well plates. Proliferation was assessed by incorporation of $[^3H]$thymidine (1 µCi/well), which was added for the last 16 h of each culture, or by CFSE (Invitrogen) dilution by loading cells according to the manufacturer's protocol.

Metaphase fluorescent in situ hybridization. Metaphase chromosome preparations were derived from 10 µg/ml LPS (Sigma-Aldrich)-activated splenocytes. RP23-77A8 (SLAM, CD84, and Ly108) *B6* BAC clone was labeled with the biotin-nick translation method (Roche) and hybridized overnight with the metaphase preparations. Specific hybridization signals were detected by incubating the hybridized slides in fluoresceinated streptavidin followed by DAPI counterstaining.

Online supplemental material. Fig. S1 shows the generation and description of $Ly108^{-/-}$ [*B6*] mice and the boundaries of the *129* segments in congenic $Ly108^{-/-}$ [*B6* × *129*] and *B6.129chr1b* mice. Fig. S2 supports protein expression experiments in Fig. 2 A. Fig. S3 explains the genetic difference between haplotype 1 and haplotype 2 mouse strains, which leads to the selective expression of Ly108-H1. Fig. S4 describes the *Sle1b*.BACLy108-H1 and *Sle1b*xBACLy108-H1 strains. Fig. S5 supports autoantibody and in vitro proliferation data of Fig. 6. Table S1 describes cellular changes in aged *B6*, *Sle1b*, and *Sle1b*.BACLy108-H1 mice. Table S2 provides information about the congenic breakpoint SNP markers. Online supplemental material is available at http://www.jem.org/cgi/content/full/jem.20101653/DC1.

We thank Drs. Arlene Sharpe, Jose Ramon Regueiro, and George Tsokos for thoughtful discussions and a critical review of the manuscript and Dr. Lisa Westerberg for technical advice.

This work was supported by grants from the National Institutes of Health (DK073339 and AI-065687 to C. Terhorst).

The authors have no conflicting financial interest.

Author contributions: M. Keszei, C. Detre, S.T. Rietdijk, and C. Terhorst designed research. M. Keszei, C. Detre, S.T. Rietdijk, P. Muñoz, S.B. Berger, S. Calpe, G. Liao, W. Castro, and Y.-Y. Wu performed research. M. Keszei, S.T. Rietdijk, X. Romero, S. Calpe, A. Julien, and N. Wang generated critical reagents. D.-M. Shin, J. Sancho, M. Zubiaur, H.C. Morse III, L. Morel, and P. Engel contributed new reagents or analytic tools. M. Keszei, C. Detre, and S.T. Rietdijk analyzed data. C. Terhorst wrote the paper, and M. Keszei, C. Detre, and S.B. Berger helped to edit and revise the manuscript.

Submitted: 10 August 2010
Accepted: 15 February 2011

REFERENCES

Black, D.L. 2003. Mechanisms of alternative pre-messenger RNA splicing. *Annu. Rev. Biochem.* 72:291–336. doi:10.1146/annurev.biochem.72.121801.161720

Bygrave, A.E., K.L. Rose, J. Cortes-Hernandez, J. Warren, R.J. Rigby, H.T. Cook, M.J. Walport, T.J. Vyse, and M. Botto. 2004. Spontaneous autoimmunity in 129 and C57BL/6 mice-implications for autoimmunity described in gene-targeted mice. *PLoS Biol.* 2:E243. doi:10.1371/journal.pbio.0020243

Calpe, S., N. Wang, X. Romero, S.B. Berger, A. Lanyi, P. Engel, and C. Terhorst. 2008. The SLAM and SAP gene families control innate and adaptive immune responses. *Adv. Immunol.* 97:177–250. doi:10.1016/S0065-2776(08)00004-7

Cannons, J.L., H. Qi, K.T. Lu, M. Dutta, J. Gomez-Rodriguez, J. Cheng, E.K. Wakeland, R.N. Germain, and P.L. Schwartzberg. 2010. Optimal germinal center responses require a multistage T cell:B cell adhesion process involving integrins, SLAM-associated protein, and CD84. *Immunity.* 32:253–265. doi:10.1016/j.immuni.2010.01.010

Carlucci, F., J. Cortes-Hernandez, L. Fossati-Jimack, A.E. Bygrave, M.J. Walport, T.J. Vyse, H.T. Cook, and M. Botto. 2007. Genetic dissection of spontaneous autoimmunity driven by 129-derived chromosome 1 Loci when expressed on C57BL/6 mice. *J. Immunol.* 178:2352–2360.

Carlucci, F., L. Fossati-Jimack, I.E. Dumitriu, Y. Heidari, M.J. Walport, M. Szajna, P. Baruah, O.A. Garden, H.T. Cook, and M. Botto. 2010. Identification and characterization of a lupus suppressor 129 locus on chromosome 3. *J. Immunol.* 184:6256–6265. doi:10.4049/jimmunol.0901463

Chang, S., L. Yang, Y.M. Moon, Y.G. Cho, S.Y. Min, T.J. Kim, Y.J. Kim, W. Patrick, H.Y. Kim, and C. Mohan. 2009. Anti-nuclear antibody reactivity in lupus may be partly hard-wired into the primary B-cell repertoire. *Mol. Immunol.* 46:3420–3426. doi:10.1016/j.molimm.2009.07.014

Chen, Y.F., C. Cuda, and L. Morel. 2005. Genetic determination of T cell help in loss of tolerance to nuclear antigens. *J. Immunol.* 174:7692–7702.

Cohen, P.L., and M.A. Maldonado. 2003. Animal models for SLE. *Curr. Protoc. Immunol.* Chapter 15:Unit 15.20.

Crispín, J.C., B.T. Keenan, M.D. Finnell, B.L. Bermas, P. Schur, E. Massarotti, E.W. Karlson, L.M. Fitzgerald, S. Ergin, V.C. Kyttaris, et al. 2010a. Expression of CD44 variant isoforms CD44v3 and CD44v6 is increased on T cells from patients with systemic lupus erythematosus and is correlated with disease activity. *Arthritis Rheum.* 62:1431–1437.

Crispín, J.C., V.C. Kyttaris, C. Terhorst, and G.C. Tsokos. 2010b. T cells as therapeutic targets in SLE. *Nat Rev Rheumatol.* 6:317–325. doi:10.1038/nrrheum.2010.60

Cunninghame Graham, D.S., T.J. Vyse, P.R. Fortin, A. Montpetit, Y.C. Cai, S. Lim, T. McKenzie, L. Farwell, B. Rhodes, L. Chad, et al. 2008. Association of LY9 in UK and Canadian SLE families. *Genes Immun.* 9:93–102. doi:10.1038/sj.gene.6364453

Detre, C., M. Keszei, X. Romero, G.C. Tsokos, and C. Terhorst. 2010. SLAM family receptors and the SLAM-associated protein (SAP) modulate T cell functions. *Semin. Immunopathol.* 32:157–171. doi:10.1007/s00281-009-0193-0

Fraser, C.C., D. Howie, M. Morra, Y. Qiu, C. Murphy, Q. Shen, J.C. Gutierrez-Ramos, A. Coyle, G.A. Kingsbury, and C. Terhorst. 2002. Identification and characterization of SF2000 and SF2001, two new members of the immune receptor SLAM/CD2 family. *Immunogenetics.* 53:843–850. doi:10.1007/s00251-001-0415-7

Graham, R.R., S.V. Kozyrev, E.C. Baechler, M.V. Reddy, R.M. Plenge, J.W. Bauer, W.A. Ortmann, T. Koeuth, M.F. González Escribano, B. Pons-Estel, et al. 2006. A common haplotype of interferon regulatory factor 5 (IRF5) regulates splicing and expression and is associated with increased risk of systemic lupus erythematosus. *Nat. Genet.* 38:550–555. doi:10.1038/ng1782

Hogarth, M.B., J.H. Slingsby, P.J. Allen, E.M. Thompson, P. Chandler, K.A. Davies, E. Simpson, B.J. Morley, and M.J. Walport. 1998. Multiple lupus susceptibility loci map to chromosome 1 in BXSB mice. *J. Immunol.* 161:2753–2761.

Howie, D., F.S. Laroux, M. Morra, A.R. Satoskar, L.E. Rosas, W.A. Faubion, A. Julien, S. Rietdijk, A.J. Coyle, C. Fraser, and C. Terhorst. 2005. Cutting edge: the SLAM family receptor Ly108 controls T cell and neutrophil functions. *J. Immunol.* 174:5931–5935.

Kanta, H., and C. Mohan. 2009. Three checkpoints in lupus development: central tolerance in adaptive immunity, peripheral amplification by innate immunity and end-organ inflammation. *Genes Immun*. 10:390–396. doi:10.1038/gene.2009.6

Kim, J.R., S.O. Mathew, R.K. Patel, R.M. Pertusi, and P.A. Mathew. 2010. Altered expression of signalling lymphocyte activation molecule (SLAM) family receptors CS1 (CD319) and 2B4 (CD244) in patients with systemic lupus erythematosus. *Clin. Exp. Immunol*. 160:348–358. doi:10.1111/j.1365-2249.2010.04116.x

Kono, D.H., R.W. Burlingame, D.G. Owens, A. Kuramochi, R.S. Balderas, D. Balomenos, and A.N. Theofilopoulos. 1994. Lupus susceptibility loci in New Zealand mice. *Proc. Natl. Acad. Sci. USA*. 91:10168–10172. doi:10.1073/pnas.91.21.10168

Kumar, K.R., L. Li, M. Yan, M. Bhaskarabhatla, A.B. Mobley, C. Nguyen, J.M. Mooney, J.D. Schatzle, E.K. Wakeland, and C. Mohan. 2006. Regulation of B cell tolerance by the lupus susceptibility gene Ly108. *Science*. 312:1665–1669. doi:10.1126/science.1125893

Mohan, C., E. Alas, L. Morel, P. Yang, and E.K. Wakeland. 1998. Genetic dissection of SLE pathogenesis. Sle1 on murine chromosome 1 leads to a selective loss of tolerance to H2A/H2B/DNA subnucleosomes. *J. Clin. Invest*. 101:1362–1372.

Morel, L. 2010. Genetics of SLE: evidence from mouse models. *Nat Rev Rheumatol*. 6:348–357. doi:10.1038/nrrheum.2010.63

Morel, L., X.H. Tian, B.P. Croker, and E.K. Wakeland. 1999. Epistatic modifiers of autoimmunity in a murine model of lupus nephritis. *Immunity*. 11:131–139. doi:10.1016/S1074-7613(00)80088-6

Morel, L., K.R. Blenman, B.P. Croker, and E.K. Wakeland. 2001. The major murine systemic lupus erythematosus susceptibility locus, Sle1, is a cluster of functionally related genes. *Proc. Natl. Acad. Sci. USA*. 98:1787–1792. doi:10.1073/pnas.031336098

Morris, S.C., P.L. Cohen, and R.A. Eisenberg. 1990. Experimental induction of systemic lupus erythematosus by recognition of foreign Ia. *Clin. Immunol. Immunopathol*. 57:263–273. doi:10.1016/0090-1229(90)90040-W

Muyrers, J.P., Y. Zhang, G. Testa, and A.F. Stewart. 1999. Rapid modification of bacterial artificial chromosomes by ET-recombination. *Nucleic Acids Res.* 27:1555–1557. doi:10.1093/nar/27.6.1555

Nambiar, M.P., E.J. Enyedy, V.G. Warke, S. Krishnan, G. Dennis, G.M. Kammer, and G.C. Tsokos. 2001. Polymorphisms/mutations of TCR-zeta-chain promoter and 3′ untranslated region and selective expression of TCR zeta-chain with an alternatively spliced 3′ untranslated region in patients with systemic lupus erythematosus. *J. Autoimmun*. 16:133–142. doi:10.1006/jaut.2000.0475

Osoegawa, K., M. Tateno, P.Y. Woon, E. Frengen, A.G. Mammoser, J.J. Catanese, Y. Hayashizaki, and P.J. de Jong. 2000. Bacterial artificial chromosome libraries for mouse sequencing and functional analysis. *Genome Res.* 10:116–128.

Peck, S.R., and H.E. Ruley. 2000. Ly108: a new member of the mouse CD2 family of cell surface proteins. *Immunogenetics*. 52:63–72. doi:10.1007/s002510000252

Rozzo, S.J., T.J. Vyse, C.G. Drake, and B.L. Kotzin. 1996. Effect of genetic background on the contribution of New Zealand black loci to autoimmune lupus nephritis. *Proc. Natl. Acad. Sci. USA*. 93:15164–15168. doi:10.1073/pnas.93.26.15164

Snow, A.L., R.A. Marsh, S.M. Krummey, P. Roehrs, L.R. Young, K. Zhang, J. van Hoff, D. Dhar, K.E. Nichols, A.H. Filipovich, et al. 2009. Restimulation-induced apoptosis of T cells is impaired in patients with X-linked lymphoproliferative disease caused by SAP deficiency. *J. Clin. Invest*. 119:2976–2989.

Subramanian, S., Y.S. Yim, K. Liu, K. Tus, X.J. Zhou, and E.K. Wakeland. 2005. Epistatic suppression of systemic lupus erythematosus: fine mapping of Sles1 to less than 1 mb. *J. Immunol*. 175:1062–1072.

Tsuzaka, K., I. Fukuhara, Y. Setoyama, K. Yoshimoto, K. Suzuki, T. Abe, and T. Takeuchi. 2003. TCR zeta mRNA with an alternatively spliced 3′-untranslated region detected in systemic lupus erythematosus patients leads to the down-regulation of TCR zeta and TCR/CD3 complex. *J. Immunol*. 171:2496–2503.

Wagner, E.J., and M.A. Garcia-Blanco. 2001. Polypyrimidine tract binding protein antagonizes exon definition. *Mol. Cell. Biol*. 21:3281–3288. doi:10.1128/MCB.21.10.3281-3288.2001

Walter, J.E., F. Rucci, L. Patrizi, M. Recher, S. Regenass, T. Paganini, M. Keszei, I. Pessach, P.A. Lang, P.L. Poliani, et al. 2010. Expansion of immunoglobulin-secreting cells and defects in B cell tolerance in *Rag*-dependent immunodeficiency. *J. Exp. Med*. 207:1541–1554. doi:10.1084/jem.20091927

Wandstrat, A.E., C. Nguyen, N. Limaye, A.Y. Chan, S. Subramanian, X.H. Tian, Y.S. Yim, A. Pertsemlidis, H.R. Garner Jr., L. Morel, and E.K. Wakeland. 2004. Association of extensive polymorphisms in the SLAM/CD2 gene cluster with murine lupus. *Immunity*. 21:769–780. doi:10.1016/j.immuni.2004.10.009

You, Y., Z. Wang, G.H. Deng, Y. Liu, and F. Hao. 2010. Detection and functional evaluation of -262A/T and -188A/G polymorphisms of SLAM gene in patients with systemic lupus erythematosus. *J. Rheumatol*. 37:2268–2272. doi:10.3899/jrheum.091390

Zhong, M.C., and A. Veillette. 2008. Control of T lymphocyte signaling by Ly108, a signaling lymphocytic activation molecule family receptor implicated in autoimmunity. *J. Biol. Chem*. 283:19255–19264. doi:10.1074/jbc.M800209200